Equilibrium Isotope Effect on Ternary Complex Formation of [1-^{18}O]Oxamate with NADH and Lactate Dehydrogenase†

Ewa Gawlita,‡ Piotr Paneth,‡ and Vernon E. Anderson*,§

Institute of Applied Radiation Chemistry, Technical University, 90-924 Lodz, Poland, Department of Biochemistry, Case Western Reserve University, Cleveland, Ohio 44106-4935, and Department of Chemistry, Brown University, Providence, Rhode Island 02912

Received January 9, 1995⊗

ABSTRACT: An equilibrium isotope effect on association of [1-^{18}O]oxamate to form a ternary complex with lactate dehydrogenase and NADH of 0.9840 ± 0.0027 has been measured by equilibrium dialysis and whole molecule isotope ratio mass spectrometry. Semiempirical calculations of vibrational frequencies using various models for solvent were shown to predict an inverse equilibrium isotope effect on association. However, the calculated effect cannot be directly attributed to one specific normal mode or vibrational force constant. Analysis of the carboxylate interaction with the guanidinium ion showed that the ionic interaction increased the torsional force constant for rotation about the carbon−carbon bond of oxamate. The minimum energy geometry for oxamate interacting with methyl guanidinium predicts that the plane of the oxamate carboxylate will be at an oblique angle to the plane defined by the guanidinium nitrogens. The combination of experimental and calculated equilibrium isotope effects on association holds the potential to improve the characterization of the interaction of ligands with protein active sites.

Changes in structure and electronic configuration of a substrate upon binding to the active site of an enzyme have been of considerable interest because of the potential application of such data to rational drug design. Vibrational and electronic spectroscopies have provided the best evidence for electronic rearrangement in substrates bound at active sites. The seminal studies on the polarization of the substrate carbonyls in triose phosphate isomerase (Belasco & Knowles, 1980) and citrate synthase (Kurz & Drysdale, 1987; Kurz *et al.*, 1985) established IR and ^{13}C NMR as being able to detect significant changes in the electronic structure. More recently, detailed Raman studies of substrates bound to lactate dehydrogenase (LDH)[1] (Deng *et al.*, 1989a,b, 1992) and ketosteroid isomerase (Austin *et al.*, 1992) have demonstrated the potential to examine several different vibrational modes, while the careful studies of Tonge and Carey have unequivocally established the catalytic importance of the polarization of substrate carbonyls in the hydrolysis of the acyl−enzyme intermediate in chymotrypsin (Tonge & Carey, 1992).

Following these observations of altered vibrational spectra on substrate binding to an enzyme active site, the dogma that substrate binding is unaffected by isotopic substitution required closer inspection. Indeed, a study by one of us, using both scintillation counting and whole molecule mass spectrometry to determine isotope ratios, demonstrated a significant normal isotope effect on association of [4-^{3}H]-NAD^+ and [4-^{2}H]NAD^+ with LDH (LaReau *et al.*, 1989). More recently, we have taken advantage of the precision of CO_2 isotope ratio mass spectrometry to detect heavy atom kinetic isotope effects on association of phosphoenolpyruvate with pyruvate kinase and phosphoenolpyruvate carboxylase (Gawlita *et al.*, 1995). Here we present an experimental determination of an ^{18}O equilibrium isotope effect on formation of the ternary LDH−NADH−oxamate complex, $^{18}K_A$,[2] and correlate the experimental value with a predicted value based on semiempirical calculations of the oxamate vibrational spectra in solvent and when bound to the active site in the structure determined by X-ray crystallography (Abad-Zapatero *et al.*, 1987; Wigley *et al.*, 1992).

Oxamate, an isosteric and isoelectronic analogue of pyruvate, was used in kinetic studies of LDH and shown to trigger the same conformational changes during the ternary complex formation as induced by substrate. The comparison of crystal structures of the apoenzyme, the binary LDH−NADH complexes (Chandrasenkhar *et al.*, 1973; Adams *et al.*, 1973), and the ternary complex with oxamate and NADH (Abad-Zapatero *et al.*, 1987) made it possible to infer the function of specific amino acid residues in catalysis and binding. Subsequent site-directed mutagenesis studies permitted identification of Arg-169 as the residue which is almost solely responsible for the binding of the carboxylate of pyruvate or lactate (Clarke *et al.*, 1986). The guanidinium group of this residue forms two hydrogen bonds with the carboxylate group of the substrate. The significance of the bifurcated H-bond was tested by mutating Arg-169 to lysine. This R169K mutation left the NADH binding essentially unchanged, but reduced the affinity of the enzyme for pyruvate to 0.05% of that of the wild type. This corresponds to the loss of about 5 kcal/mol in binding energy, which was attributed to the formation of two charged hydrogen bonds (Hart *et al.*, 1987a,b).

† Supported by grants from the National Institutes of Health to V.E.A. (GM 36562) and P.P. (TW00262). V.E.A. is a fellow of the Sloan Foundation (1990−1992). The experimental portion of this work was performed by E.G. in the Brown University Chemistry Department Laboratories.

‡ Technical University.

§ Case Western Reserve University.

⊗ Abstract published in *Advance ACS Abstracts,* April 15, 1995.

[1] Abbreviations: HEPES, 4-(2-hydroxyethyl)-1-piperazineethanesulfonic acid; LDH, lactate dehydrogenase.

[2] The isotope effect nomenclature of Northrop (1982) as expanded by Cleland (1982) is used. A leading superscript indicates an isotope effect on the following parameter, computed as the ratio of light to heavy; e.g., $^{18}K_A$ is the ratio of the equilibrium association constants for [^{16}O]oxamate and [1-^{18}O]oxamate.

0006-2960/95/0434-6050$09.00/0

While the interaction between Arg-169 and the oxamate carboxylate is clearly a very strong interaction, a general method for determining the strength of H-bond interactions is experimentally difficult. Fersht and his co-workers' classic studies on tyrosyl-tRNA synthetase demonstrated that H-bonds between amino acid side chains and substrates can be thermodynamically favorable or unfavorable, depending on how strong the comparable hydrogen bonds to solvent are (Leatherbarrow & Fersht, 1987). While these and many other site-directed mutagenesis studies have been interpreted as yielding information on the strength of individual hydrogen bonds, the inherent limitation of these studies is the inability to account for other structural alterations introduced by any mutation. Consequently, it would be desirable to have a direct physical method of quantifying the strength of that interaction. Detection of hydrogen bonds by vibrational spectroscopy in enzyme−ligand systems, while feasible, requires detection of the O−H stretching frequencies in the presence of water. This is a severe limitation, and while isotope-edited difference Raman spectroscopy may succeed, the identification of a hydrogen-bonded stretch has not been demonstrated. Isotope effects, on the other hand, can potentially reveal the same changes in frequencies of hydrogen bonds without the obstacles encountered in diffeence spectroscopies. We hypothesized that examining isotope effects on association might lead to a general method of quantifying the enthalpy of H-bond formation.

The size of the observed isotope effect on ligand binding is commensurate with the strength of the hydrogen bond in which the labeled atoms are involved. This is an extension of Badger's rule, which states that as the strength of the hydrogen bond increases, the frequency of the O−H stretch decreases (Jencks, 1969). Labeling of the hydrogen atoms is usually employed in spectroscopic detection of hydrogen bonds, but in the case of carboxylic acids, where the hydrogens are readily exchangeable with the solvent, ^{18}O-labeling provides a useful substitute, albeit with the technical requirement for higher precision in the determination of the smaller isotope effect. Whole molecule isotope ratio mass spectrometry combined with negative chemical ionization has been demonstrated to have the precision required for determination of heavy atom isotope effects on binding (Bahnson & Anderson, 1991).

These considerations led us to select the carboxylate oxygens of oxamate as an interesting site for the measurement of an isotope effect on enzyme−substrate association. The obvious advantage of such a choice was that any measurable isotope effect on the association of oxamate with LDH can almost certainly be ascribed to the formation of the bifurcated hydrogen bond between the oxamate carboxylate and the guanidinium group of Arg-169. This, coupled with modeling of the active site, might permit a correlation of the strength of the hydrogen bond with the magnitude of the observed isotope effect on binding. While such a correlation was not found for guanidinium:carboxylate ion pairs, the investigation of the isotope effect led to the identification of an unexpected nonplanar geometry of interaction between the carboxylate and guanidinium groups.

MATERIALS AND METHODS.

Materials. Oxamic acid (free acid), oxamic acid ethyl ester, [^{14}C]oxalic acid, ethyl acetate, NADH as the disodium salt, LDH (E.C. 1.1.1.27) as the salt-free lyophilized powder (type XI from rabbit muscle), and 4-(2-hydroxyethyl)-1-piperazineethanesulfonic acid (HEPES) as the free acid were purchased from Sigma. Pentafluorobenzyl bromide, acetone, absolute ethanol, and ammonia gas were from Aldrich. [^{18}O]-Water (98 atom %) was from Cambridge Isotopes. The PLGC dialysis membrane (MW cutoff, 10 000) was purchased from Millipore. All chemicals were the highest possible grade and were used without further purification.

Synthesis of [1-^{18}O]Oxamate. Oxamate ethyl ester (3 mmol) was hydrolyzed with 30 mmol of [^{18}O]water (98 atom %) to introduce ^{18}O into one position of the oxamate carboxyl group. Anhydrous potassium phosphate (tribasic) was used to attain basic pH (about 12). The resulting product was then diluted with natural-abundance oxamate so that the final ^{18}O enrichment was about 50% as determined by the isotope ratio analysis. This synthesis introduces at most one ^{18}O atom per carboxylate.

Synthesis of [U-^{14}C]Oxamate. The synthesis of [U-^{14}C]-oxamate was a modification of that presented by L. C. Coppet (1866). [^{14}C]Oxalic acid (0.3 mmol, 10.4 mCi/mmol) was dissolved in 2 mL of absolute ethanol, acidified with concentrated HCl, and heated at 40 °C for 1 h. Water (1 mL) was then added, and the diethyl ester of [^{14}C]oxalic acid was extracted with three equal volumes of ether. The ether extracts were pooled, dried under a stream of dry nitrogen, and subsequently redissolved in 1 mL of ethanol. The solution was placed in an ice bath, and ammonia gas was bubbled through the solution until a white solid precipitated (about 1 h). The remaining ethanol was removed under a nitrogen stream. The purity of the product oxamate was tested using a Hewlett-Packard 5988A quadrupole mass spectrometer equipped with a direct-insertion probe. Under positive chemical ionization (PCI) conditions both oxamic acid and oxamide could be detected as protonated molecular ions at *m/z* 90 and 89, respectively. In order to avoid masking of peaks due to oxamide by much more abundant oxamic acid peaks, the samples were treated with concentrated NaOH prior to drying on the direct-insertion probe tip, which prevented the volatilization of oxamate but had no effect on oxamide. Mass spectrometric analysis of the product treated in such a way did not reveal peaks due to oxamide.

Equilibrium Dialysis. All binding equilibria were established in a dialysis cell consisting of two 1-mL chambers separated by a PLGC 10 000 MW cutoff membrane. Each chamber was filled with 0.8−1.0 mL of buffered solution. LDH (0.8 mM active sites), 8 mM NADH, 2 mM [1-^{18}O]-oxamate, and 5 μM [^{14}C]oxamate in 100 mM HEPES buffer, pH 7.0, was allowed to equilibrate for 15−20 min and then dialyzed against the same volume and concentration of NADH in HEPES for 8−12 h at 4 °C. The concentrations of oxamate on both sides of the dialysis cell were monitored by scintillation counting of 10-μL aliquots from both sides of the dialysis chamber as described for the determination of the fraction of oxamate bound (see below). After about 8 h, no further change in oxamate concentration in either chamber of the dialysis cell was observed. The solutions from each chamber were then removed using a syringe and processed in parallel as described below.

Fraction Bound Determination. Equal aliquots, typically 25 μL, from each chamber were counted in order to determine the fraction of [^{14}C]oxamate bound to the enzyme.

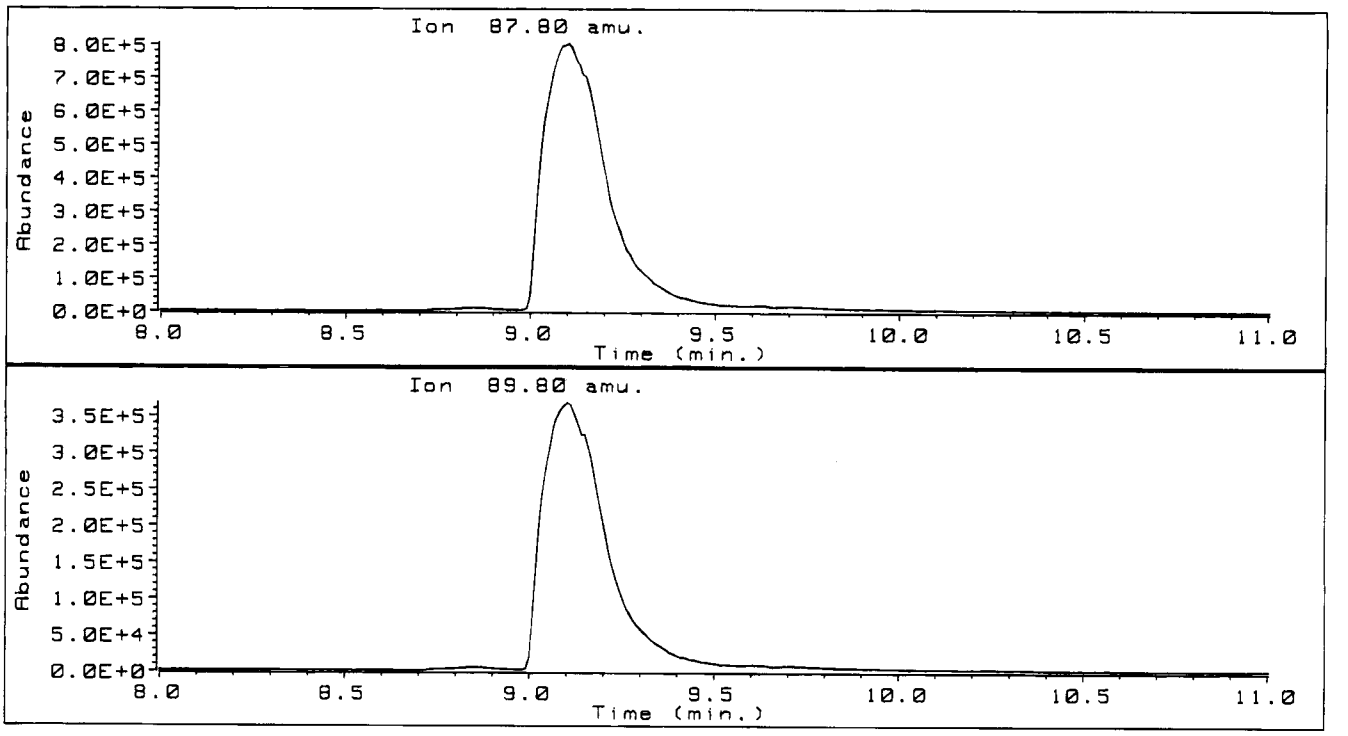

FIGURE 1: Selected ion chromatograms of [1-^{16}O]:[1-^{18}O]oxamate, *m/z* 87.8 and 89.8, attributed to the ^{16}O- and ^{18}O-labeled oxamates, respectively. The important features of the chromatograms for precise isotope ratio measurements are the width of the peak relative to the cycle time of 100 ms, the identical appearance of both chromatograms, and the minimal background.

The aliquots were added to 10 mL of Ecolume scintillation fluid and counted two or three times to a standard deviation of less than 0.5% (typically 10−20 min) using a Beckman LS5000TD scintillation counter. The fraction of the inhibitor bound to the enzyme, f_B, was determined using eq 1:

$$f_B = \frac{c_M - c_F}{c_M + c_F} \quad (1)$$

where c_M and c_F are numbers of counts of equal volume aliquots from the chamber containing LDH and from the chamber without enzyme, respectively.

Esterification with Pentafluorobenzyl Bromide. The enzyme present in one sample was heat denatured by placing it in a heating block at 60 °C for 10 min and subsequently removed by centrifugation in an Eppendorf centrifuge at 12000*g* for 10 min. Oxamate contained in the supernatant, as well as in the sample coming from the other chamber of the dialysis cell, was then esterified with pentafluorobenzyl bromide (Hunt & Crow, 1978; Trainor & Vouros, 1987). The pH of both samples was brought to about 4.5 by addition of 1 mL of 100 mM phosphate buffer, pH 4.5, and additional titration with 1 M HCl. Acetone (2 mL) and 10 μL of pentafluorobenzyl bromide were added, and the samples were allowed to react at 70 °C for 5 h. The pentafluorobenzyl ester of oxamate was then extracted five times with equal volumes of ethyl acetate; the ethyl acetate extracts were pooled and dried under a stream of dry nitrogen. The residue was redissolved in 100 μL of ethyl acetate and subjected to mass spectral analysis. A control sample containing only the original oxamate was also derivatized and analyzed in the same way.

Isotopic Ratio Analysis. The M + 1/M isotope ratios of the oxamate pentafluorobenzyl esters were determined using a Hewlett-Packard 5988A quadrupole mass spectrometer interfaced to an HP 5890 gas chromatograph. The mass spectrometer was tuned in the NCI mode using perfluorotributylamine as a standard. The source temperature was kept at 250 °C, and the methane pressure was kept between 0.5 and 1.0 Torr. Under the GC column temperature gradient of 80 to 200 °C at 10 °C/min, the oxamate pentafluorobenzyl ester eluted between 9.0 and 9.5 min. The mass spectrometer was operated in the single ion monitoring (SIM) mode for negative ions at *m/z* 88, 89, and 90 (formed by dissociative electron capture by the pentafluorobenzyl, pfb, moiety) corresponding to the $(M - pfb)^-$, $(M + 1 - pfb)^-$, and $(M + 2 - pfb)^-$ ions respectively. Each ion was monitored for 50 ms, which ensured well-defined sampling of the GC peaks. The sample injections were done automatically using an HP 7673 automatic liquid sampler connected to the gas chromatograph. An average of six injections per sample were acquired with at least two blank injections between different samples. The resulting peaks were integrated after subtraction of the baseline over a range of 9.0−10.0 min, and the ^{18}O/^{16}O ratios were determined from the ratio of peaks at *m/z* 90 and 88. Examples of the selected ion chromatograms for the ions *m/z* 88 and 90 are shown in Figure 1. The corresponding mass spectrum is shown in Figure 2.

Calculations. The ^{18}O equilibrium isotope effect on the association constant ($^{18}K_A$) can be determined by eq 2:

$$^{18}K_A = R_F/R_B \quad (2)$$

where R_F and R_B are the isotopic ratios measured for oxamate bound to the enzyme and that free in solution, respectively. R_F can be measured directly from the sample obtained from the chamber without LDH, but R_B must be calculated either from R_M, which is the isotopic ratio actually measured for oxamate from the enzyme-containing side of the dialysis cell,

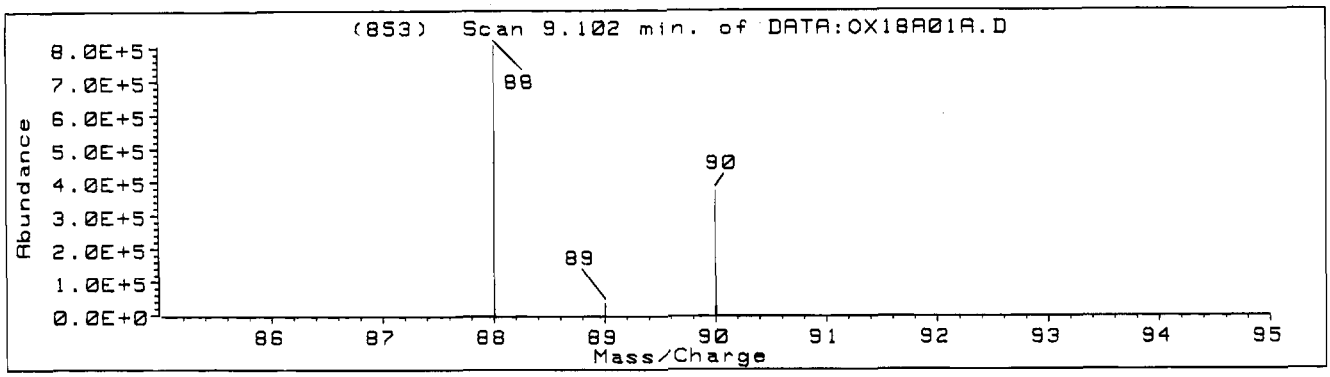

FIGURE 2: Negative chemical ionization mass spectrum of [1-^{18}O]:[1-^{16}O]oxamate. For precise isotope ratio measurements, the M − 1 peak, i.e., *m/z* 87, is less than 0.2% of the parent ion at *m/z* 88.

or from the isotope ratio of the starting material, R_0, and a mass balance. By measuring and comparing the results for sets of the three isotopic ratios R_F, R_0, and R_B and from the control showing that interfering peaks in the gas chromatogram arose from the presence of LDH in the sample, we determined that R_0 could be measured with greater confidence than R_M, which was found to be on average 1% smaller than predicted from the R_0 and R_B ratios. Therefore, the R_B isotopic ratios were calculated using eq 3:

$$R_B = R_0/f_B - R_F(1 - f_B)/f_B \quad (3)$$

Theoretical Modeling. A detailed description and outcome of these calculations is presented elsewhere (except for the Langevin dipole model calculations) (Gawlita *et al.*, 1994). Here we only illustrate these calculations with examples of the best and worst correlations to the experimental value.

Theoretical evaluation of the equilibrium isotope effect requires a comparison of the vibrational spectra of oxamate bound at the LDH active site with that of oxamate in aqueous solution. MOPAC, version 6.0 (Steward, 1990), from the Quantum Chemistry Program Exchange, was used for the calculations of the ternary LDH−NADH−oxamate complex and of oxamate in aqueous solution. The active site model with bound oxamate and NADH truncated at the 5″-phospho moiety was based on the crystal structure of the ternary complex of dogfish LDH with NADH and oxamate available as Brookhaven Protein Data Bank file 1LDM (Abad-Zapatero *et al.*, 1987). The Insight II molecular graphics package (Biosym) was used to select the relevant amino acid residues and extract their coordinates from the original file. A 5-Å radius centered on the oxamate molecule contained the following amino acids: His-193, Arg-106, Arg-169, Asn-138, and the truncated NADH. Analysis of the most likely protonation states of the oxamate carboxyl group as well as ionizable portions of the four amino acid residues and the NADH molecule at pH 7.0 resulted in applying a net charge of −3. The model contained 132 atoms, but only coordinates of atoms of the oxamate ion were subjected to optimization, while the frame of the active site was kept rigid. After the geometry optimization, the vibrational analysis was carried out. Using the AM1 Hamiltonian on all atoms of the model correctly reproduced the observed value of the isotope effect.

In order to evaluate the vibrational properties of oxamate in solution, several methods of accounting for the effect of solvent water molecules were used. One of the methods which correctly reproduced the isotope effect was to explicitly include molecules of solvent in a solvation sphere; the entire ensemble of molecules has been referred to as a "supermolecule" (Kitaura & Morokuma, 1976; Cramer & Truhlar, 1991; Luzkhov & Warshel, 1992). In a 5-Å radius around the oxamate molecule, 22 TIP4P water molecules (Jorgensen *et al.*, 1983) were generated with the "soak" option in the Insight software. The geometry optimization was then carried out with the −1 net charge from the oxamate applied to the supermolecule.

Alternative methods of including the effects of solvent in semiempirical calculations limit the quantum mechanical treatment to the solute, while the effect of the solvent is represented by effective potentials which are included in the solute Hamiltonian. The self-consistent reaction field (SCRF) method with the AM1 Hamiltonian and COSMO has proven to yield the best results among those methods; a solvation method (SM2) (Cramer & Truhlar, 1991) and a Langevin dipole model (LD) (Warshel & Russell, 1984) failed to reproduce experimental data. All of these methods treat solvent as a continuum of given macroscopic and microscopic properties, including dielectric constant and different shapes of cavity. The LD method was used from within the SIBIQ program modified to include isotopic masses (Bliznyuk *et al.*, 1994). Predefined properties of the aqueous solution, based mostly on dielectric constant, polarizability, density, dipole moment, and interaction energy between water molecules, were used during the geometry optimization with varied minimal and maximal radii of the solvent sphere. Under none of these conditions was it possible to achieve a calculated value of the oxygen equilibrium isotope effect close to the experimentally observed value.

Following vibrational analysis, equilibrium isotope effects were calculated from eq 4 (Melander, 1960) at 277 K:

$$\frac{K_{16}}{K_{18}} = \left(\frac{M_{16}^P}{M_{18}^P}\frac{M_{18}^S}{M_{16}^S}\right)^{3/2}\left(\frac{A_{16}^P B_{16}^P C_{16}^P}{A_{18}^P B_{18}^P C_{18}^P}\frac{A_{18}^S B_{18}^S C_{18}^S}{A_{16}^S B_{16}^S C_{16}^S}\right)^{1/2} \prod_i^{3n-6}\frac{\sinh^{1/2} u_{i(18)}^P}{\sinh^{1/2} u_{i(16)}^P}\prod_i^{3n-6}\frac{\sinh^{1/2} u_{i(16)}^S}{\sinh^{1/2} u_{i(18)}^S} \quad (4)$$

In eq 4, M is the molecular mass; A, B, and C are the principal moments of inertia; n is the number of atoms; and $u_i = h\nu_i/kT$. The subscripts 16 and 18 refer to the ^{16}O- and ^{18}O-labeled oxamate, and the superscripts S and P refer to the initial and final states, respectively. Information necessary for calculation of the isotope effect was extracted from

Table 1: Determination of $^{18}K_A$[a]

expt	f_B	R_F (±SD)[b]	R_0 (±SD)	$^{18}K_A$
1	0.528	0.48182(0.00092)	0.48642(0.00225)	0.9822
2	0.516	0.46029(0.00053)	0.46298(0.00043)	0.9888
3	0.54[c]	0.45314(0.00134)	0.45723(0.00224)	0.9835
4	0.554	0.45896(0.00048)	0.46334(0.00246)	0.9830
5	0.377	0.42997(0.00166)	0.43286(0.00193)	0.9824

[a] R_F and R_0 are the free and initial [1-^{18}O]oxamate/[^{16}O]oxamate isotope ratios determined by whole molecule isotope ratio mass spectrometry as described under Materials and Methods. f_B is the fraction of oxamate bound as ternary complex in the LDH-containing chamber of the dialysis. $^{18}K_A$ was calculated from eq 2. [b] SD reflects the standard deviation of the multiple determinations of the given isotope ratio. [c] For this set of measurements the exact value of f_B was not determined explicitly, but estimated using the fraction bound from other sets of experiments carried out under identical conditions. This value has a very limited influence on the final value of the determined isotope effect.

the MOPAC output file and used directly in eq 4 with the aid of the program ISOEFF.[3]

Torsional Force Constant Calculation. The force field in MOPAC calculations is generated in Cartesian coordinates, making it impossible to determine the force constants for a given internal coordinate, such as a bond stretching or a rotation about a dihedral angle. To estimate the increase in a torsional force constant for a carboxylate that could be attributed to forming a bifurcated H-bond with guanidinium, the energy of a carboxylate system was geometry optimized while the dihedral angle was constrained using AM1 through a HYPERCHEM (Hypercube) interface. After the geometry optimization, the dihedral constraint was removed and the energy was determined. This generates the energy as a function of the dihedral angle as shown in Figure 3. Fitting the data to a parabola, eq 5, allows the force constant, k_{tor}, for the different torsional systems to be estimated.

$$E = k_{tor}(\theta - \theta_e)^2 \quad (5)$$

Three oxamate systems were examined. (1) Oxamate in vacuo provides an intrinsic k_{tor}, due to steric interaction with the other atoms of oxamate. (2) Oxamate ion paired with methylguanidinium or H-bonded to two water molecules was used to identify the increase in torsional force constant from distortion of H-bonds. For both the guanidinium and two water molecule models, the minimum energy conformation did not maintain coplanarity of the carboxylate and guanidinium or the two water molecules. Separate calculations constraining these groups to be coplanar were performed with an improper dihedral used as the constraint. The constraint was removed prior to calculating the energy of the fixed system. (3) The effect of the interactions of oxamate with the LDH active site on the torsional force constant were determined with the residues described above.

RESULTS

The experimental $^{18}K_A$ values for oxamate forming a ternary LDH−NADH−oxamate complex are given in Table 1. The average value (of five determinations) of $^{18}K_A$ was 0.9840 ± 0.0027. The reported error was calculated as the standard deviation of all determinations. Under the conditions used, i.e., $f_B > 0.5$ and both measured isotope ratios varying by less than 1%, the precision of the isotope ratio measurements is the major source of error. We have previously shown that the precision of isotope ratios measured by NCI of pentafluorobenzyl esters is sufficient for determination of heavy atom isotope effects (Bahnson & Anderson, 1991; Anderson *et al.*, 1994). The enhanced precision of our procedure is due to three main factors: (1) The presence of background contamination of the source is negligible in NCI, as only molecules with high electron affinity generate negative ions, whereas in standard electron impact ionization there is always a variable background at any mass. (2) The NCI mass spectrum of pentafluorobenzyl ester of oxamate, and most other carboxylates, yields only the fragment generated by dissociative electron capture, minimizing background from the sample and eliminating potential isotope effects on ionization and fragmentation. (3) Our chromatographic procedure, which elutes the peak as a broad Gaussian to permit over 50 determinations and multiple sequential injections, allows an actual standard deviation of the individual determination to be determined.

Table 2: Calculated Frequencies Sensitive to ^{18}O Substitution

aqueous solution[a] (cm^{-1})		LDH active site[b] (cm^{-1})	
^{16}O	^{18}O	^{16}O	^{18}O
256.7	252.4	469.4	464.7
511.4	505.1	545.5	535.9
520.2	514.6	556.7	550.7
657.5	647.5	637.8	633.6
871.3	860.2	647.5	639.6
1613.2	1560.7	1544.9	1540.0
2052.7	2017.5	1551.2	1546.8
		1602.8	1597.2
		1621.4	1602.9
		1634.5	1621.5
		1644.9	1638.9
		2094.1	2067.4
		2103.3	2094.2

[a] AM1 calculation with explicit water molecules. [b] AM1 calculation of oxamate optimized structure at the LDH active site incorporating the residues as described under Materials and Methods.

The computational methods used in our studies satisfactorily reproduced the experimental observation of an inverse $^{18}K_A$. Employing the gas-phase approximation for oxamate bound in the ternary LDH complex active site and a number of alternative methods for the simulations of solvent effects, we obtained the vibrational spectra of oxamate in the different environments. The frequencies that showed a significant shift when ^{18}O was introduced into oxamate are tabulated in Table 2. The following values of $^{18}K_A$ were calculated from the frequencies using eq 4. In the supermolecule approach with an explicit definition of water molecules to simulate the aqueous solution, the calculated $^{18}K_A$ was 0.986. The SCRF and COSMO methods, which model the solvent as a continuum by modification of the Hamiltonian, generated calculated $^{18}K_A$ values of 0.984 and 0.994, respectively. The calculated values are all consistent with the experimentally observed inverse effect.

The results of the calculations of the torsional force constants for rotation about the oxamate C−C bond are shown in Figure 3. The rotational force constant calculated for oxamate at the active site will produce vibrational frequencies of ca. 200 cm^{-1}. Figure 3A shows the increase in the torsional force constant when interactions with two

[3] The FORTRAN program ISOEFF may be obtained by request from P. Paneth at ppaneth1@plearn.edu.pl.

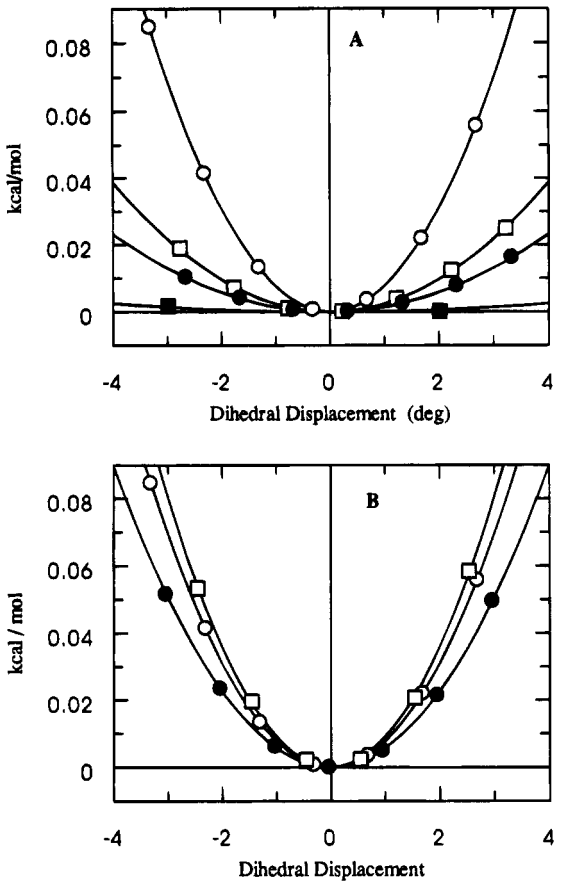

FIGURE 3: Calculation of the torsional potential for rotation about the oxamate C−C bond: (A) In a vacuum (■), H-bonded to two coplanar water molecules (●), in an ion pair with methyl guanidinium constrained to be coplanar (□), and in the LDH active site (○); and (B) H-bonded to two water molecules (●), in an ion pair with methyl guanidinium (□), and in the LDH active site (○). The energies were calculated by generating an equilibrium minimum energy structure and subsequently fixing the oxamate N−C−C−O dihedral at values of $\pm n°$ for $n = 1-3$, from the equilibrium dihedral value. The energy of the system was then recalculated without reoptimizing the geometry. The potential wells for each system were translated to the origin.

coplanar water molecules, a coplanar guanidinium, or the LDH active site residues are included in the calculation. Clearly the interaction with H-bond donors increases the force constant, and the active site is a more restricted environment than that imposed by either coplanar H-bonded model. If the increase in torsional frequency associated with transfer from vacuum to the active site were the only difference between the free and bound states, an $^{18}K_A$ of 0.994 would be predicted. The magnitude of the active site rotational barrier, however, is closely reproduced by the nonplanar water and guanidinium H-bonded models. This suggests that it is the close approach of atoms above and below the plane of the carboxylate and not the strength and angular dependence of the H-bonds that is responsible for the increase in the calculated rotational force constant.

DISCUSSION

Inverse Isotope Effects on Association. The significant inverse value of the equilibrium isotope effect, $^{18}K_A$, indicates that the heavier isotope tends to concentrate in the enzyme-bound state because the carboxyl C−O bond becomes

Scheme 1

Scheme 2

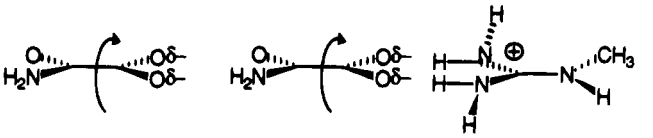

"stiffer" when bound to the enzyme. This isotope effect contrasts with the kinetic equilibrium isotope effects reported for the association of [2-^{18}O]phosphoenolpyruvate with two different enzymes (Gawlita *et al.*, 1995), because these effects were measured at equilibrium and reflect differences in the ground-state environment of the isotopically substituted bond between that in aqueous solution and that when bound at the enzyme active site. The fact that the isotope effect is inverse is not surprising. The partitioning of [^{18}O]-formate out of water into other phases is accompanied by an inverse effect of up to 0.995 (Hermes *et al.*, 1984). With formate, the vibrations are simplified since there is no substituent besides hydrogen on the carboxylate. This inverse effect may come from a decrease in the nucleophilic solvation of the carbonyl carbon as detected in the partitioning of α-^{2}H carbonyl compounds (Kovach & Quinn, 1983). The nucleophilic solvent water molecule reduces the bond order between the carbonyl carbon and oxygen. However, the magnitude of the reported effect is significantly larger than 0.995, and additional explanations must be sought.

Semiempirical Calculation of Isotope Effects. To observe an inverse isotope effect, at least one of the vibrational force constants associated with the isotopically substituted bond must be increased in the ternary complex with LDH and NADH. The process of binding can be visualized as the extraction of a substrate or inhibitor from the more random aqueous solution to the more defined interaction present at the enzyme active site. Prior to the binding process, the oxygens of the carboxyl group were involved in hydrogen bonds with water molecules. After binding, these hydrogen bonds were replaced by the bifurcated H-bonds with the guanidinium group of Arg-169. Consequently, we anticipated that the measured $^{18}K_A$ would result from differences in strength and directionality of somewhat unordered hydrogen bonds of the carboxylate group with water molecules and the highly directional hydrogen bonds formed with the guanidinium group in the enzyme active site.

Semiempirical calculations offer the potential of identifying the normal modes of vibration that generate the inverse $^{18}K_A$. In internal coordinates, we can picture the carboxylates as having several different idealized vibrational degrees of freedom, including symmetric and antisymmetric stretches, an O−C−O bending mode, and rotation about the C-1−C-2 bond as shown in Schemes 1 and 2. While the degrees of freedom are visualized as internal coordinate motions, the calculated force fields are expressed in Cartesian coordinates

and consequently cannot be immediately correlated with individual internal coordinate motions, i.e., a specific force constant for bond stretching or rotation about a bond.

The initial attempt at identifying the calculated normal modes in solution and in the ternary complex associated with the carboxylate was to determine whether the mode was sensitive to substitution with ^{18}O. This is analogous to normal mode assignments in vibrational spectroscopy where identification of normal modes relies on spectra of isotopically substituted molecules. For each normal mode frequency MOPAC identifies the atom pairs which undergo the largest displacement from equilibrium and whether the motion is parallel or perpendicular to the bond between the atoms. At high frequency, above 1600 cm^{-1}, the vibrations are largely identifiable as specific bond stretches. Most of the lower frequency vibrations are more complex normal modes consisting of the relative motions of a larger number of atoms; i.e., simple bond angle bending and dihedral torsions are coupled and not identifiable as unique frequencies.

In this way the 26.7-cm^{-1} decrease in frequency in ^{18}O oxamate was used to assign the 2094-cm^{-1} normal mode in the ternary complex to the antisymmetric stretching frequency of the carboxylate C−O bonds. The corresponding frequencies in aqueous solution were predicted to be lower by all employed methods. While unanticipated, this phenomenon is understandable if the H-bonds to both carboxylate oxygens are stronger in the ternary complex. The antisymmetric stretch necessarily shortens one H-bond while the other lengthens. If the strength of the ternary complex H-bond has a stronger distance dependence than in aqueous solution, the result will be that demonstrated by the calculations. These stretching modes of oxamate are shown in Scheme 1.

The identification of the carboxylate symmetric stretching frequency has proven more difficult. In the range of 1600–1630 cm^{-1} there were several ^{18}O-sensitive frequencies. The observation of these "split" frequencies makes it infeasible to compare the calculated difference between solution and the ternary complex with the experimentally observed values for pyruvate, where a minimal 8-cm^{-1} shift was obtained when the ternary adduct complex was formed (Deng *et al.*, 1989a). While a direct numerical comparison is not possible because of the systematically high vibrational frequencies in semiempirical calculations,[4] the observation and calculation of an inverse $^{18}K_A$ is entirely consistent with the very small decrease in carboxylate stretching frequencies observed in the Raman spectra.

An important feature of the calculated vibrational characteristics of oxamate in both environments is that a number of low vibrational frequencies were also found to be sensitive to the carboxylate ^{18}O substitution as shown in Table 2. Such additional low frequencies of vibrations are experimentally observable, for example, in dimers of carboxylic acids (Pinchas & Laulicht, 1971) and interpreted as arising from hydrogen bonds. The ability of the employed methods to reproduce these frequencies as well as the fact that they are sensitive to the carboxylate ^{18}O substitution make them likely candidates for the Cartesian normal mode expression of the calculated isotope effect.

Geometry of Oxamate−Guanidinium Interaction. Because the strength of the bifurcated guanidinium H-bond is required for the high-affinity association of oxamate, we investigated whether the interaction would generate an increase in the torsional force constant for rotation about the oxamate C−C bond shown below.

The minimum energy structure for oxamate ion paired with methyl guanidinium has rotated the carboxylate so that the planes defined by the carboxylate and guanidinium are twisted by 63° as shown in Figure 3A. This twist permits the guanidinium dipole to come closer to the carboxylate dipole. This consideration is not overly simplistic since Scheiner (1994) has shown from *ab initio* calculations that the angular dependence of H-bonds can be inferred from considering the functional group dipoles. The growing realization that H-bond strength at enzyme active sites (Gerlt & Gassman, 1993) depends on the relative proton affinity of the H-bond donor and acceptor (Epley & Drago, 1967) suggests that the H-bonds between the guanidinium and the carboxylate will be weak because of the disparity in pK_a between the two functional groups. Thus our observation that the structure optimizes the electrostatic interactions at the expense of forming linear H-bonds is less surprising. The results in Figure 3 show that the interaction of oxamate with the guanidinium does enhance the rotational force constant, relative to water. However, the increased torsional force constant is not a function of maintaining linear H-bonds.

In the twisted conformation, some of the restoring force that enhances the torsional force constant comes from van der Waals repulsion. To isolate the contribution of the bifurcated H-bonds to a planar guanidinium−oxamate interaction, the geometry of the guanidinium−oxamate interaction was optimized while guanidinium and oxamate were constrained to remain coplanar by restraining an improper dihedral consisting of the terminal three atoms of the guanidinium and the carboxylate carbon. The torsional force constants obtained with planar H-bonds are shown in Figure 3A, while Figure 3B shows the stiffer torsional potential obtained with the energetically preferred twisted conformation.

Since the preferred geometry of carboxylates with guanidinium groups in high-resolution crystal structures has this same twisted orientation (Singh *et al.*, 1987), the enhanced torsional force constant may be common to carboxylate−guanidinium ion pairs in enzyme active sites. In an analysis of the geometry of interacting arginine−carboxylate ion pairs in high-resolution protein crystal structures, Singh *et al.* (1987) identified a twist of between 30°−50° as being the most probable when the carboxylate carbon was within 22.5° of the guanidinium plane. For LDH, in the highest resolution structure, 1LDM (Abad-Zapatero, 1987), the angle between the carboxylate and guanidinium planes is 12°, while in the structure of the lactyl−NAD complex, 5LDH, the carboxylate and guanidinium are coplanar (Grau *et al.*, 1981). In the NAD^+ pyruvate adduct structure, 3LDH (White *et al.*, 1977), the angle is 50°, while in the NADH−oxamate ternary complex with the *B. stearothermophilus* LDH, 1LDN (Wigley *et al.*, 1992), the four active sites were refined separately, and the angles ranged from 0° to 33°. The variation in the observed angles for LDH is potentially due to differences in the complexes; bias introduced during the refinement, with

[4] While the vibrations in semiempirical calculations are systematically high, the isotope effects are dependent on the ratio of frequencies for the light and heavy atom species, so that the systematic error does not affect the isotope effect calculation.

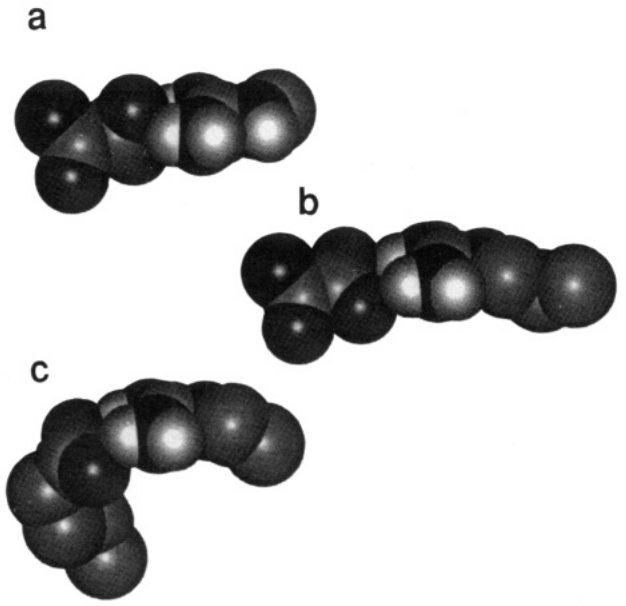

FIGURE 4: Geometry of carboxylate−guanidinium interactions. (A) The minimum energy oxamate−methylguanidinium structure. (B) The interaction of the myristate carboxylate with guanidinium in the intestinal fatty acid binding protein (1ICM). (C) The interaction of oxamate with Arg-106C in the *B. stearothermophilus* LDH (1LDN). All atoms are represented as spheres drawn with their van der Waals radii; nitrogen, oxygen, carbon, and hydrogen are drawn with decreasing darkness. Only the guanidinium hydrogens are included.

the resolution of the structures being insufficient to determine an unequivocal relative conformation; or librational freedom such that a set geometry does not exist.

In a very high resolution structure of intenstinal fatty acid binding protein, 1ICM (January, 1994, revision; Eads *et al.*, 1993; Scapin *et al.*, 1992), where the fatty acid carboxylate is complexed with an arginine, the angle between the planes is 54° (Figure 4). Other twisted structures can be found in high-resolution structures of a phosphonate tetrahedral intermediate bound to carboxypeptidase (7CPA) (Kim & Lipscomb, 1991) and *N*-phosphonoacetyl-L-aspartate bound to aspartate transcarbamylase (8ATC) (Ke *et al.*, 1988). In the carboxypeptidase structure, the carboxylate interaction is with Arg-145 and is important for making the enzyme an exopeptidase. The two carboxylates of the *N*-phosphonoacetyl-L-aspartate both interact with distinct guanidiniums of arginine at angles of 39° and 19°. All atomic coordinates were obtained from the Brookhaven Protein Data Base (Bernstein *et al.*, 1977; Abola *et al.*, 1987). Thus the twisted orientation of the oxamate and guanidinium groups reflected in the AM1 optimized geometry and shown in Figure 4 is observed in high-resolution crystal structures and is statistically the most favorable orientation. This provides some confidence that the torsional energy wells shown in Figure 3 and the isotope effect calculations are not artifacts of the AM1 Hamiltonian.

Prevalence of Equilibrium Isotope Effects on Association. In a recent study, Loh and Markley measured the fractionation factor for most of the amide protons in staphylococcal nuclease by ^{1}H NMR (Loh & Markley, 1994). They identified fractionation factors ranging from 0.4 to over 1.15. This large range of fractionation factors corroborates the thesis of this work, i.e., that specific interactions in macromolecular complexes have a detectable effect on isotopic fractionation. The ^{2}H fractionation factors observed by NMR correlated with the structural location of the amide, with solvent-exposed amides having near unity fractionation factors and those in α-helices having normal fractionation factors. The ability to detect ^{18}O isotope effects on association is significant in that it points the way to potential measurements of H-bond strength between ligand and active site and a better understanding of the solvation environment of bound ligands. It also requires that the interpretation of heavy atom isotope effect measurements of near unity be treated with caution because there is a demonstrated possibility that they arise from molecular changes other than that observed during the chemical reaction.

ACKNOWLEDGMENT

We would like to thank Jennifer Grant for assistance in writing a C program to calculate the angle between the planes defined by guanidinium and carboxylate groups using coordinates from the protein data base.

REFERENCES

Abad-Zapatero, C., Griffith, J. P., Sussman, J. L., & Rossmann, M. G. (1987) *J. Mol. Biol. 198*, 445.

Abola, E. E., Bernstein, F. C., Bryant, S. H., Koetzle, T. F., & Weng, J. (1987) Protein Data Bank, in *Crystallographic Databases—Information Content, Software Systems, Scientific Applications* (Allen, F. H., Bergerhoff, G., & Sievers, R., Eds.) pp 107−132, Data Commission of the International Union of Crystallography, Cambridge.

Adams, M. J., Liljas, A., & Rossmann, M. G. (1973) *J. Mol. Biol. 76*, 519.

Anderson, S. R., Anderson, V. E., & Knowles, J. R. (1994) *Biochemistry 33*, 10545.

Austin, J. C., Kuliopulos, A., Mildvan, A. S., & Spiro, T. G. (1992) *Protein Sci. 1*, 259.

Bahnson, B. J., & Anderson, V. E. (1991) *Biochemistry 30*, 5894.

Belasco, J. G., & Knowles, J. R. (1980) *Biochemistry 19*, 472−477.

Bernstein, F. C., Koetzle, T. F., Williams, G. B., Meyer, E. F., Jr., Brice, M. D., Rodgers, J. R., Kennard, O., Shimanouchi, T., & Tasumi, M. (1977) *J. Mol. Biol. 112*, 532.

Bliznyuk, A. A., Pachkovsky, S. S., & Voityuk, A. A. (1994) SIBIQ, ver. 1.0.6.

Chandrasenkhar, K., McPherson, A., Jr. & Adams, M. J. (1973) *J. Mol. Biol. 76*, 503.

Clarke, A. R., Wigley, D. B., Chia, W. N., Barstow, D. A., Atkinson, T., & Holbrook, J. J. (1986) *Nature 324*, 699.

Cleland, W. W. (1982) *CRC Crit. Rev. Biochem. 13*, 385.

Coppet, L. C. (1866) *Annalen 137*, 105.

Cramer, C. J., & Truhlar, D. G. (1991) *J. Am. Chem. Soc. 113*, 8305.

Deng, H., Zheng, J., Burgner, J., & Callender, R. (1989a) *Proc. Natl. Acad. Sci. U.S.A. 86*, 4484.

Deng, H., Zheng, J., Sloan, D., Burgner, J., & Callender, R. (1989b) *Biochemistry 28*, 1525.

Deng, H., Zheng, J., Sloan, D., Burgner, J., & Callender, R. (1992) *Biochemistry 31*, 5085.

Eads, J., Sacchettini, J. C., Kromminga, A., & Gordon, J. I. (1993) *J. Biol. Chem. 268*, 26375.

Epley, T. D., & Drago, R. S. (1967) *J. Am. Chem. Soc. 89*, 5770.

Gawlita, E., Anderson, V. E., & Paneth, P. (1994) *Eur. Biophys. J. 23*, 353.

Gawlita, E., Caldwell, W. S., O'Leary, M. H., Paneth, P., & Anderson, V. E. (1995) *Biochemistry 34*, 2577.

Gerlt, J. A., & Gassman, P. G. (1993) *J. Am. Chem. Soc. 115*, 11552.

Grau, U. M., Trommer, W. E., & Rossman, M. G. (1981) *J. Mol. Biol. 151*, 289.

Hart, K. W., Clarke, A. R., Wigley, D. B., Chia, W. N., Barstow, D. A., Atkinson, T., & Holbrook, J. J. (1987a) *Biochem. Biophys. Res. Commun. 146*, 346.
Hart, K. W., Clarke, A. R., Wigley, D. B., Waldman, A. D. B., Chia, W. N., Barstow, D. A., Atkinson, T., Jones, J. B., & Holbrook, J. J. (1987b) *Biochem. Biophys. Acta 914*, 294.
Hermes, J. D., Morrical, S. W., O'Leary, M. H., & Cleland, W. W. (1984) *Biochemistry 23*, 5479.
Hunt, D. F., & Crow, F. W. (1978) *Anal. Chem. 50*, 1781.
Jencks, W. P. (1969) *Catalysis in Chemistry and Enzymology*, McGraw-Hill, New York.
Jorgensen, W. L., Chandrasekhas, J., Madura, J. D., Impley, R. W., & Klein, M. L. (1983) *J. Chem. Phys. 79*, 926.
Ke, H., Lipscomb, W. N., Cho, Y., & Honzatko, R. B. (1988) *J. Mol. Biol. 204*, 725.
Kim, H., & Lipscomb, W. N. (1991) *Biochemistry 30*, 8171.
Kitaura, K., & Morokuma, K. (1976) *Int. J. Quantum Chem. 10*, 325.
Kovach, I. M., & Quinn, D. M. (1983) *J. Am. Chem. Soc. 105*, 1947.
Kurz, L. C., & Drysdale, G. R. (1987) *Biochemistry 26*, 2623.
Kurz, L. C., Ackerman, J. J., & Drysdale, G. R. (1985) *Biochemistry 24*, 452.
LaReau, R. D., Wan, W., & Anderson, V. E. (1989) *Biochemistry 28*, 3619.
Leatherbarrow, R. J., & Fersht, A. R. (1987) in *Enzyme Mechanism* (Page, M. I., Ed.) pp 78−96, CRC Press, Boca Raton, FL.
Loh, S. N., & Markley, J. L. (1994) *Biochemistry 33*, 1029−1036.
Luzkhov, V., & Warshel, A. (1992) *J. Comput. Chem. 11*, 199.
Northrop, D. B. (1982) *Methods Enzymol. 87*, 607.
Pinchas, S., & Laulicht, I. (1971) in *Infrared Spectra of Labelled Compounds*, Academic Press, London and New York.
Scapin, G., Gordon, J. I., & Sacchettini, J. C. (1992) *J. Biol. Chem. 267*, 4253.
Scheiner, S. (1994) *Acc. Chem. Res. 27*, 402−408.
Singh, J., Thornton, J. M., Snarey, M., & Campbell, S. F. (1987) *FEBS Lett. 224*, 161−171.
Steward, J. J. P. (1990) *J. Comput. Chem. 11*, 543.
Tonge, P. J., & Carey, P. R. (1992) *Biochemistry 31*, 9122.
Trainor, T. M., & Vouros, P. (1987) *Anal. Chem. 59*, 601.
Warshel, A., & Russell, S. T. (1984) *Q. Rev. Biophys. 17*, 283.
White, J. L., Hackert, M. L., Buehner, M., Adams, M. J., Ford, G. C., Lentz, P. J., Jr., Smiley, I. E., Steindel, S. J., & Rossmann, M., (1976) *J. Mol. Biol. 102*, 759.
Wigley, D. B., Gamblin, S. J., Turkenburg, J. P., Dodson, E. J., Piontek, K., Muirhead, H., & Holbrook, J. J. (1992) *J. Mol. Biol. 223*, 317.

BI950040T